Frequency-Dependent UWB Channel Characteristics in Office Environments

Jinwon Choi, *Student Member, IEEE*, Noh-Gyoung Kang, Yu-Suk Sung, Jun-Sung Kang, and Seong-Cheol Kim, *Member, IEEE*

***Abstract*—This paper reports frequency-dependent ultrawideband (UWB) channel characteristics. Measurements were performed in 103 receiver locations of six different office environments. From the measured data, the effect of frequency on the pathloss properties of a UWB signal is analyzed. After analyzing the pathloss behavior to propagation environments, the pathloss exponent variation models are developed in various environments as a function of frequency. Based on these models, pathloss prediction is performed, and the accuracy of the prediction is compared with those of existing pathloss models. In addition, the frequency-dependent UWB channel correlation characteristics are investigated. For the frequency correlation statistics of the UWB channel, double-slope models representing correlation coefficients are established with and without line-of-sight (LOS) paths. Using these correlation models, a channel gain estimation algorithm is proposed. The performance of the proposed estimation algorithm is evaluated with estimation parameters, and it is confirmed that the proposed estimation algorithm has better performance than the conventional algorithm using a linear interpolation algorithm.**

***Index Terms*—Channel estimation, empirical channel modeling, frequency-dependent channel, ultrawideband (UWB).**

I. Introduction

FOR short-range high-data-rate wireless communication, ultrawideband (UWB) communication systems have strong advantages such as low complexity, low cost, resistance to severe multipath fading, and fine time resolution. Since the Federal Communication Commission announced the regulation of UWB transmission, development of commercial UWB systems has been very active [1]. From a low-data-rate system, such as a localization sensor network, to a high-speed service, such as multiband orthogonal frequency-division multiplexing (MB-OFDM), the UWB technique can be adopted for various wireless systems. To develop efficient UWB systems, research should deal with the propagation properties of UWB signals and the issues associated with the large bandwidth involved in UWB systems. Furthermore, the underlying interference problem caused by the large bandwidth must be resolved for UWB systems to coexist with other existing communication systems. With regard to channel models for UWB systems, the literature has reported diverse properties of UWB systems [2]–[7]. However, channel characterization in the frequency domain is insufficient, although the wide frequency band is the most distinguishable feature of UWB systems [8]–[10].

In this paper, we empirically investigated the frequency-dependent characteristics of the UWB channel. By performing frequency-dependent channel characterization, diverse UWB communications on various frequency bands can effectively be designed [11], [12]. The frequency-dependent UWB channel characteristics are analyzed in two distinct viewpoints: 1) the effect of frequency on the pathloss properties and 2) the channel gain correlation properties in the frequency domain. The office environment is selected for channel characterization since the office is one of the most probable environments in which multiple wireless devices transmit high-speed data signals. To investigate the effect of the wide frequency band of UWB systems, we measured the channel transfer functions at 5.8 GHz with a 1.6-GHz bandwidth for 103 receiver locations in six different office environments using the frequency sweep method. For the first part of the analysis, the pathloss properties are analyzed by considering the propagation environments and the existence of a line-of-sight (LOS) path. The proposed log–distance pathloss model parameters are the most fundamental characteristics in the development of the link budget and service coverage of UWB communications. By analyzing the variation of the pathloss exponent with frequency, a suitable pathloss exponent variation model for UWB systems for operating bandwidths of more than 500 MHz is proposed. The pathloss exponent for a subband whose bandwidth is 500 MHz increases with frequency as a linear function of frequency. Then, using this pathloss exponent function, the performance of the pathloss formula is improved. In the latter part of the analysis, correlation properties of the UWB channel in the frequency domain are analyzed. Although some works have dealt with the correlation property of the UWB pulse [13], [14], frequency-dependent correlation properties have not been investigated in detail. The frequency correlation statistics of the UWB channel are characterized with correlation coefficients as a function of frequency separation. They are expressed as double-slope linear models with a 30-MHz breakpoint for the existence of an LOS path. Using these correlation models, the channel gain estimation algorithm is proposed. In this algorithm, the unknown channel

Manuscript received May 27, 2008; revised December 16, 2008. First published February 3, 2009; current version published August 14, 2009. This work was supported in part by the Brain Korea 21 Project and in part by the IT R&D Program of the Ministry of Knowledge Economy/Institute for Information Technology Advancement under Grant 2008-F-007-01, Intelligent Wireless Communication Systems in 3 Dimensional Environment. The review of this paper was coordinated by Prof. R. C. Qiu.

J. Choi, Y.-S. Sung, J.-S. Kang, and S.-C. Kim are with the Department of Electrical Engineering, Institute of New Media and Communications, Seoul National University, Seoul 151-742, Korea (e-mail: caesar@maxwell.snu.ac.kr; sfamily@maxwell.snu.ac.kr; jskang@maxwell.snu.ac.kr; sckim@maxwell.snu.ac.kr).

N.-G. Kang is with Samsung Electronics Co., Suwon 442-742, Korea (e-mail: peterpan@maxwell.snu.ac.kr).

Color versions of one or more of the figures in this paper are available online at http://ieeexplore.ieee.org.

Digital Object Identifier 10.1109/TVT.2009.2014070

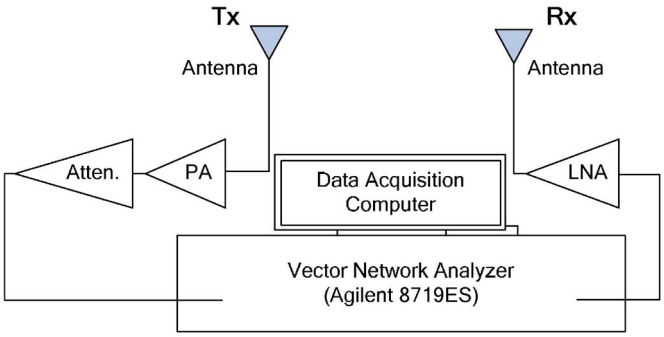

Fig. 1. Block diagram of the measurement system.

gains of intervening frequencies are estimated from known channel gains of neighboring reference frequencies using the correlation model. The performance of the proposed estimation algorithm is evaluated with the estimation parameters, number of reference frequencies, and interval between reference frequencies and compared with that of the conventional algorithm that uses a linear interpolation scheme.

This paper is organized as follows: Section II presents the channel measurement system and measurement scenario. Section III provides the effect of frequency on the pathloss properties, and Section IV shows the correlation properties of the channel gain in the frequency domain. Finally, the conclusion follows in Section V.

II. Measurement Methodology

A. Measurement System

Among the UWB channel measurement methods, we selected the frequency-domain channel sounding method for channel characterization [8], [15]. With this measurement technique, wide frequency bands are swept to measure channel frequency responses at discrete frequencies using a vector network analyzer (VNA). The VNA (Agilent 8719ES) transmits 801 discrete tones uniformly spaced from 5 to 6.6 GHz with a frequency interval of 2 MHz, and it takes 400 ms for one sweeping. This frequency interval allows us to measure multipaths with a maximum excess delay of 500 ns, and the bandwidth of 1.6 GHz gives a time resolution of less than 0.01 ns. The measurement system is described in Fig. 1. A pathloss of up to 110 dB can be measured by properly adjusting the transmit power using a power amplifier (PA), a low-noise amplifier (LNA), and a step attenuator (Atten.). The transmitting and receiving antennas are omnidirectional with a gain of 2.1 dBi, and they are mounted on the 1.6-m-high tripods. All measured data are calibrated by measured data in an anechoic chamber.

Fig. 2 shows frequency dependences of components of the measurement system, which are measured in a chamber. Measured channel data are compensated using these results, including the antenna effects in postprocessing [16].

B. Measurement Scenario

Frequency sweep measurements are carried out in six different office environments of three buildings in Seoul National University, Seoul, Korea. The locations of the transmitting and the receiving antennas are illustrated in Figs. 3 and 4, along

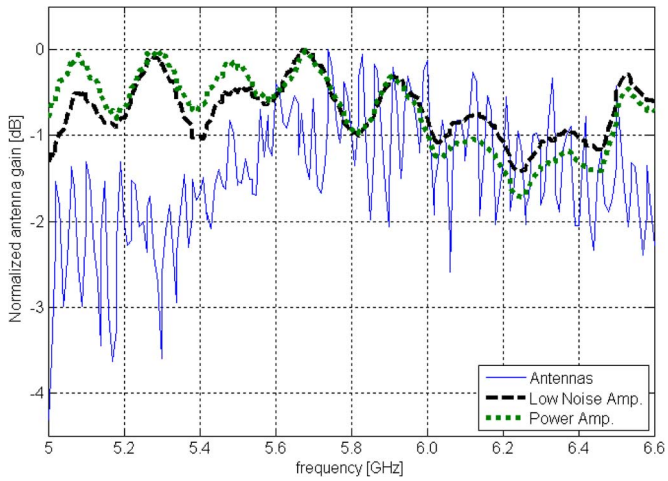

Fig. 2. Frequency dependences of components of the measurement system.

with the floor plan and the wall-type description. The location of the transmitting antenna is denoted Tx, whereas that of the receiving antenna is denoted Rx.

Environment 1 is an office on the fifth floor of a ferroconcrete building whose windows face a hill. Environments 2 and 3 are located on the second and fourth floors, respectively, of another type of ferroconcrete building whose windows face a neighboring building with metal exterior walls. Environments 1 and 2 have metal walls in the middle to divide a large office room into two small rooms, whereas the last environment consists of adjacent small office rooms and a corridor.

Environments 4 and 5 are located on the same floor with Environment 1, but they are distinctly different environments. Environment 4 consists of small rooms along a corridor with dead ends, a large lecture room, and stairs. Environment 5 is composed of two big lecture rooms and corridors. Environment 6 is the first floor of the third type of ferroconcrete building whose interior walls are made of bricks. In this environment, both ends of the corridor are blocked by glass doors. To keep the quasi-statistic channel assumption, all environments are kept stationary, and people are not allowed to move around during measurements. Out of 103 receiver locations, 49 locations have LOS paths to transmitter, and the remaining 54 locations do not. The 103 receiver locations are categorized into 12 groups according to measurement environments and the existence of a LOS path. Grouping results are summarized in Table I. At each receiver location, the receiver was moved around to nine local positions to obtain a local average, and 100 frequency responses were collected at each local position.

As a result, 900 frequency responses are taken at each receiver location. As the time interval between two consecutive responses is 1 s, 100 frequency responses were taken for 140 s at each local position.

III. Frequency-Dependent Pathloss Property of the UWB Signal

A. Empirical Parameters of Pathloss Model

To develop efficient UWB systems, the pathloss properties must first be evaluated for the analysis of the link budget and

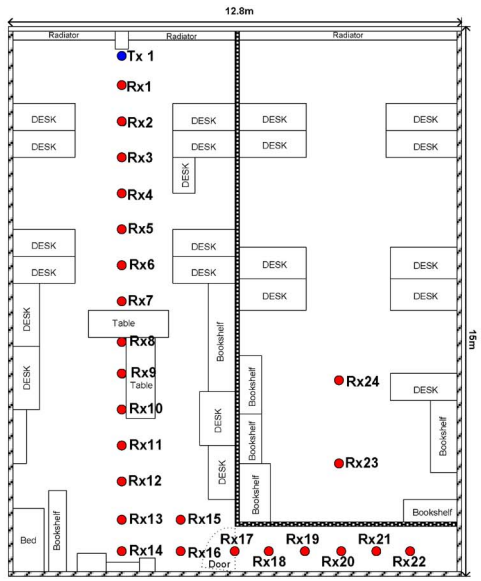

(a)

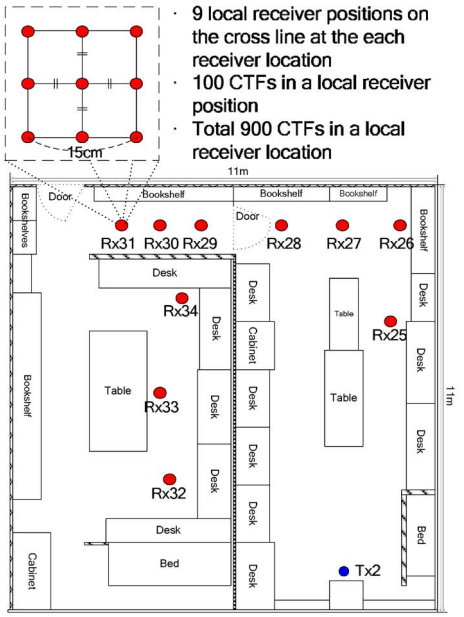

(b)

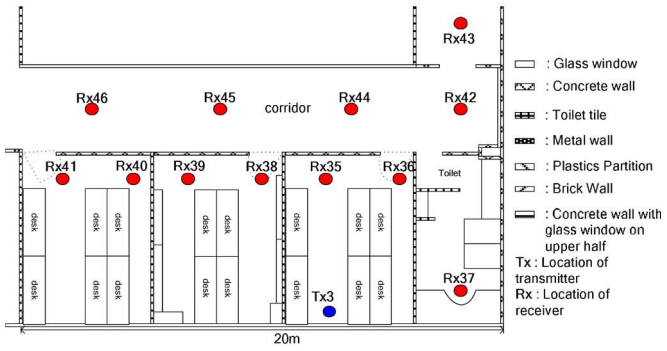

(c)

Fig. 3. Floor plans and receiver locations in office environments 1–3. (a) Environment 1. (b) Environment 2. (c) Environment 3.

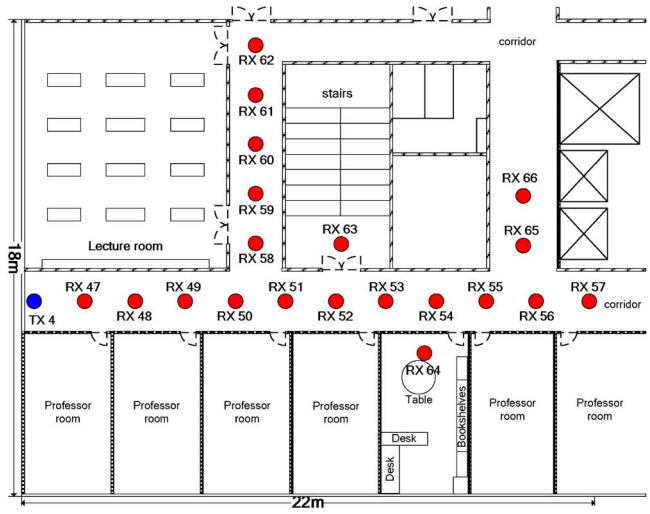

(a)

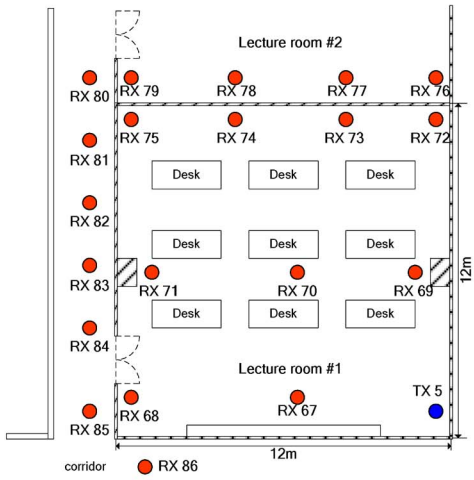

(b)

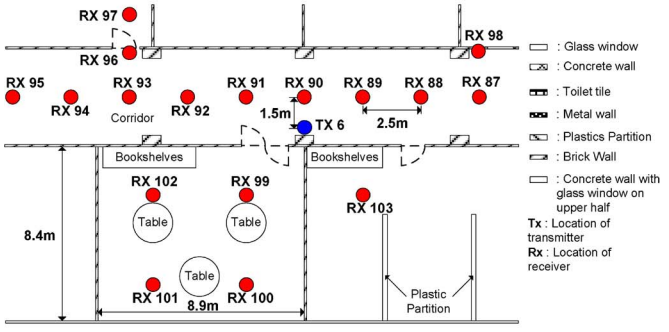

(c)

Fig. 4. Floor plans and receiver locations in office environments 4–6. (a) Environment 4. (b) Environment 5. (c) Environment 6.

possible interference prevention. For characterization of the frequency-independent UWB pathloss model, we start with the conventional log–distance pathloss formula, i.e.,

$$\mathrm{PL}(d) = \mathrm{PL}(d_0) + 10 \cdot n \cdot \log(d/d_0) + S \qquad (1)$$

where $\mathrm{PL}(d_0)$ is the pathloss at the reference distance d_0 (which is 1 m in this paper), d is the separation between the transmitter and the receiver, n is the pathloss exponent, and S is a

TABLE I
TWELVE RECEIVER GROUPS ACCORDING TO THE PROPAGATION ENVIRONMENT AND THE EXISTENCE OF A LOS PATH

E.	Group	#	Max(d) [m]	Group	#	Max(d) [m]
1	LOS 1	16	14.1	NLOS 1	8	15.7
2	LOS 2	4	9.1	NLOS 2	6	11.0
3	LOS 3	1	6.2	NLOS 3	11	15.2
4	LOS 4	11	22.0	NLOS 4	9	18.6
5	LOS 5	8	15.0	NLOS 5	12	17.3
6	LOS 6	9	12.6	NLOS 6	8	9.2

TABLE II
EMPIRICAL PATHLOSS PARAMETERS OF THE RECEIVERS

	$PL(d_0)$ [dB]	n	σ_s [dB]
LOS 1	35.596	1.58	1.025
LOS 2	37.913	1.47	1.029
LOS 4	41.729	1.27	1.647
LOS 5	40.592	1.45	1.878
LOS 6	42.502	1.98	1.645
NLOS 1	38.521	2.13	2.640
NLOS 2	41.593	2.28	4.541
NLOS 3	43.786	2.85	4.423
NLOS 4	45.529	1.85	3.673
NLOS 5	46.504	2.83	3.838
NLOS 6	47.493	3.11	2.130

zero-mean Gaussian distributed random variable (in decibels) with a standard deviation σ_s (also in decibels) [17].

PL(d), PL(d_0), and σ_s in (1) are averaged over a 1.6-GHz bandwidth, and n is computed using the minimum mean square error algorithm. Parameters for each receiver group are summarized in Table II. For LOS groups, the pathloss exponents are found to be smaller than 2, which corresponds to the free-space loss. In LOS 4, because of the waveguide effect caused by the metal wall on one side of the aisle and the brick walls on the other side of the aisle, the pathloss exponent is the smallest. For non-LOS (NLOS) locations, the pathloss exponent is about 2 for groups of NLOS 1, 2, and 4 and about three for groups of NLOS 3, 5, and 6. In the former groups, the diffracted signals around the corner of the open doors or aisles, even for a LOS path, are blocked, and multireflected signals arrive at the receiver, whereas only the transmitted signals through the walls contribute to the receiver in the latter NLOS groups.

The difference in the pathloss exponents between NLOS locations implies that the received signal strength can be increased by the existence of a diffraction path and a multiple reflection path. The shadowing factor is between 1 and 2 dB when an LOS path is guaranteed, whereas it rises to a value between 2 and 4.5 dB when an LOS path is obstructed.

B. Effect of Frequency on the Pathloss Exponent

The classical radio theory states that the pathloss is a function of wavelength [17]. The frequency-dependent pathloss property has been discussed in many literatures [3], [10]–[12], although there is a contradiction as well [18]. For existing communications using a narrow frequency bandwidth compared with the UWB, (1) is enough to show the pathloss property. However, for the UWB, a wider frequency bandwidth should be considered in the pathloss model. In this paper, the frequency-dependent pathloss is expressed using the following modified expression of (1):

$$\mathrm{PL}(d, f) = \mathrm{PL}(d_0) + 10 \cdot n(f) \cdot \log(d/d_0) + S. \quad (2)$$

For UWB systems, in particular, the MB-OFDM scheme proposes that the assigned frequency bands should be divided into subbands having bandwidths of 528 MHz [19]. To design an efficient MB-OFDM system, the effect of frequency to different frequency band UWB signals should be characterized. For that purpose, we propose a practical pathloss exponent formula to express the loss as a function of frequency. The pathloss exponent variation with frequency is characterized by taking the average of the pathloss exponent over the 500-MHz overlapped window bandwidth whose center frequency is incremented from 5.25 to 6.35 GHz in steps of 100 MHz, as shown in Fig. 5. In this paper, the pathloss exponent averaged over each subband is denoted ns_k at the kth subband, $k = 1, 2, \ldots, 12$. The variation of ns_k is expressed as a function of the center frequency of each subband. The measured ns_k's are illustrated in Fig. 6.

As shown in Fig. 6, ns_k increases with the center frequency of the subband and can be regressed as the linear function to receiver groups. A pathloss exponent variation model as a function of frequency is obtained for each receiver group, i.e.,

$$ns(f_c) = a \times f_c + b \quad (3)$$

where f_c is the center frequency of the subband (in gigahertz).

The statistical representatives of ns_k's and linear regression coefficients a and b of (3) for all receiver groups are shown in Table III. The median value of ns_k in each receiver group is almost the same as n, which is the pathloss exponent of (1), and the difference between the maximum and minimum values of ns_k is almost the same as the increasing coefficient a. Moreover, the normalized slope a/n, which is defined as the ratio of parameter a to n of (1), is analyzed. This normalized slope is about 0.2 with the LOS path and about 1.5 without the LOS path, except LOS2 and NLOS3 groups, whose a/n value is greater than 0.5. In these groups, reflected signals from the different wall material of the neighboring building for LOS2 and multireflected signals from walls of diverse materials for NLOS3 enhance the frequency selectivity. Using these statistical values, the parameters of (3) can be computed from

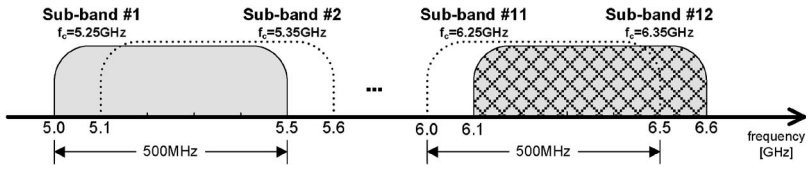

Fig. 5. Twelve subbands with bandwidths of 500 MHz.

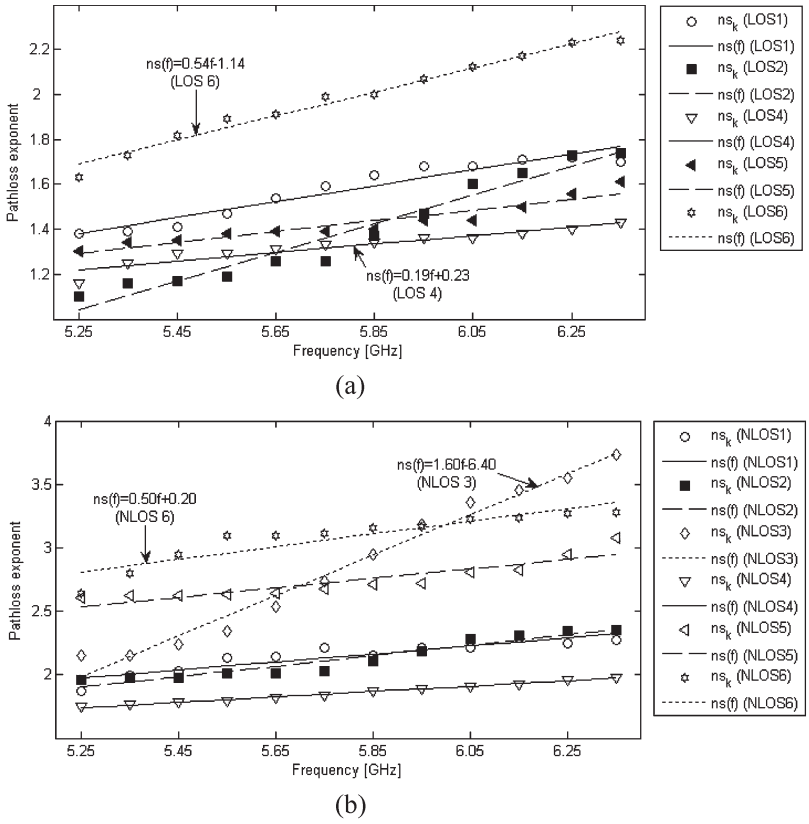

Fig. 6. ns_k's and their linear regression models grouped according to the existence of a LOS path. (a) Pathloss exponent variation for the LOS groups. (b) Pathloss exponent variation for the NLOS groups.

n of (1). From the value of the normalized slope, parameter a is computed from n and the normalized slope. Then, parameter b is determined from $ns(F_c) = n$, where F_c is the center frequency of the overall frequency band. In this paper, F_c is 5.8 GHz. From these parameters, the pathloss exponent variation model can be expressed as

$$\text{LOS locations} : ns(f_c) = 0.2n \times f_c + (1 - 0.2F_c) \qquad (4)$$

where the factor 0.2 is for LOS locations and substituted as 0.2 for NLOS locations. Exceptionally, 0.2 is changed to 0.5 in LOS2 and NLOS3 groups.

C. Performance of the Pathloss Exponent Variation Model

Using this pathloss exponent variation model, more accurate pathloss predictions can be performed to the frequency range of UWB communication to be developed. In this section, the accuracy of the pathloss formula based on the pathloss exponent variation model is compared with those of existing pathloss formulas.

As for existing pathloss formulas, the general pathloss exponent model given in (1) and the well-known frequency-dependent pathloss formula [20] are denoted PL_1 and PL_2, respectively, whereas the pathloss formula using the proposed pathloss exponent variation model in (2) is denoted PL_3. Thus

$$\begin{aligned}
&\text{PL}_1 : \text{PL}_1(d, f) = \text{PL}(d_0) + 10 \cdot n \cdot \log(d) \\
&\text{PL}_2 : \text{PL}_2(d, f) = 32.44 + 20 \log_{10} f_{\text{MHz}} + 20 \log_{10} d_{\text{km}} \\
&\text{PL}_3 : \text{PL}_3(d, f) = \text{PL}(d_0) + 10 \cdot ns(f) \cdot \log(d). \qquad (5)
\end{aligned}$$

A graphical explanation of PL_i's and their pathloss prediction error is depicted in Fig. 7. In (6), $\text{PL}(d, f)$ means the measured pathloss value (in decibels) as a function of frequency f and the separation between Tx and Rx, i.e., d. The pathloss prediction error $e_i(f)$ between PL_i ($i = 1$, 2, and 3) and $\text{PL}(d, f)$ is defined as follows:

$$e_i(d, f) = |\text{PL}_i(d, f) - \text{PL}(d, f)| \ \text{[in dB]} \quad (i = 1, 2, \text{ and } 3). \qquad (6)$$

In each receiver location, the pathloss prediction error $e_i(f)$ is averaged over the 1.6-GHz frequency range, i.e., $E_f[e_i(f)]$'s.

TABLE III
REPRESENTATIVE VALUES OF ns_k AND THEIR LINEAR REGRESSION MODEL PARAMETERS

Group	n	$MED(ns_k)$	$\triangle ns_k$	a	b	a/n
LOS1	1.58	1.62	0.32	0.35	-0.47	0.222
LOS2	1.47	1.32	0.64	0.64	-2.32	0.435
LOS 4	1.27	1.34	0.27	0.19	0.23	0.150
LOS 5	1.45	1.40	0.31	0.24	0.03	0.166
LOS 6	1.98	2.00	0.62	0.54	-1.14	0.273
LOS 1,4,5,6	-	-	-	-	-	0.203
NLOS 1	2.13	2.18	0.42	0.33	0.30	0.155
NLOS 2	2.28	2.07	0.39	0.41	-0.27	0.180
NLOS 3	2.85	2.85	1.58	1.60	-6.40	0.561
NLOS 4	1.85	1.86	0.23	0.21	0.63	0.114
NLOS 5	2.83	2.70	0.47	0.38	0.57	0.134
NLOS 6	3.11	3.13	0.64	0.50	0.20	0.161
NLOS 1,2,4,5,6	-	-	-	-	-	0.149

$MED(ns_k)$: Median value of 12 ns_k's,

Vns_k : Maximum value of ns_k -Minimum value of ns_k,
n: pathloss exponent of (1)

These results are grouped according to the existence of a LOS path and summarized in Table IV. Whether an LOS path is guaranteed or not, the pathloss prediction based on the pathloss exponent variation model shows the best performance. Once the pathloss exponent variation model is applied to the pathloss prediction, the prediction error is reduced, as compared to PL_1, i.e., 22% in LOS locations and 15% in NLOS locations, respectively. In comparison to PL_2, the prediction error is reduced by more than 55% as the proposed pathloss exponent variation model is applied.

IV. CORRELATION ANALYSIS OF THE FREQUENCY CHANNEL GAINS

For characterization of the frequency-dependent properties, the discrete frequency response of the UWB radio channel $h(f)$ is expressed as

$$h(f) = \sum_{k=1}^{801} a(f_k) e^{j\theta(f_k)} \delta(f - f_k) \tag{7}$$

where $a(f_k)$ and $\theta(f_k)$ are the amplitude and phase of the channel gain, respectively, at frequency f_k, with $\delta(\cdot)$ as the Dirac delta function. The index k indicates the sequence number of the discrete frequencies, whose interval is 2 MHz. In this experiment, f_1 is 5.0 GHz, and f_{801} is 6.6 GHz. Since the phase $\theta(f_k)$ in this experiment is modeled as a uniformly distributed random variable between 0 and 2π, the channel gain $a(f_k)$ in the voltage scale is statistically characterized.

A. Frequency Correlation Properties of the Measured Channel Gains

Since the UWB system operates in an extremely wide bandwidth compared with conventional wireless systems, it is imperative to understand the frequency correlation characteristics of UWB channels. However, the frequency correlation property of the UWB channel gain has not been investigated so far. Once the correlation model is established, the coherence bandwidth values are analyzed, and the channel gain of the intervening frequency can be estimated from neighboring known channel gains. For characterization of the frequency correlation properties, the correlation coefficient is used to represent the correlation level of the received signal amplitudes between frequency tones and is represented as [21]

$$\rho_a(\Delta f) = \frac{C_a(f, f+\Delta f)}{\sqrt{C_a(f,f)}\sqrt{C_a(f+\Delta f, f+\Delta f)}} \tag{8}$$

where $C_a(f_1, f_2) = E[\{a(f_1) - m_a(f_1)\}\{a(f_2) - m_a(f_2)\}]$, $a(f_1)$ is the amplitude of the channel gain at frequency tone f_1, and $m_a(f_1)$ is the mean of $a(f_1)$.

The correlation coefficients for the LOS and NLOS locations are shown in Fig. 8. The correlation coefficients are well fitted to the double-slope linear regression models, with the logarithm of the frequency separation as follows:

$$\rho_{a,\mathrm{LOS}}(\Delta f) = -0.224 \ln(\Delta f) + 0.843 \tag{9}$$

$$\rho_{a,\mathrm{NLOS}}(\Delta f) = -0.196 \ln(\Delta f) + 0.657. \tag{10}$$

For frequency separations below 30 MHz, the correlation coefficients for the LOS locations are larger than those for the NLOS locations. However, as the frequency separation gets larger, the correlation coefficients of the LOS locations drastically decrease and become almost the same as the coefficients of the NLOS locations beyond the frequency separation of 30 MHz. For frequency separations of 30 MHz or more, the correlation coefficients converge to 0.05 in both cases.

B. Channel Gain Estimation and Estimation Error

With these correlation properties, the unknown channel responses at intervening frequencies can be estimated from the known channel responses of neighboring frequencies. For the estimation, we defined a measured channel gain set A, which is composed of the measured channel gain at each frequency in a single frequency response. As the measured bandwidth is 1.6 GHz and the separation between adjacent frequencies is 2 MHz, the number of elements is 801. Estimation sets $\widetilde{A_L}$, based on the linear interpolation scheme, and five estimation sets $\widetilde{A_j}$'s ($j = 2, 3, \ldots, 6$), based on the correlation model, are

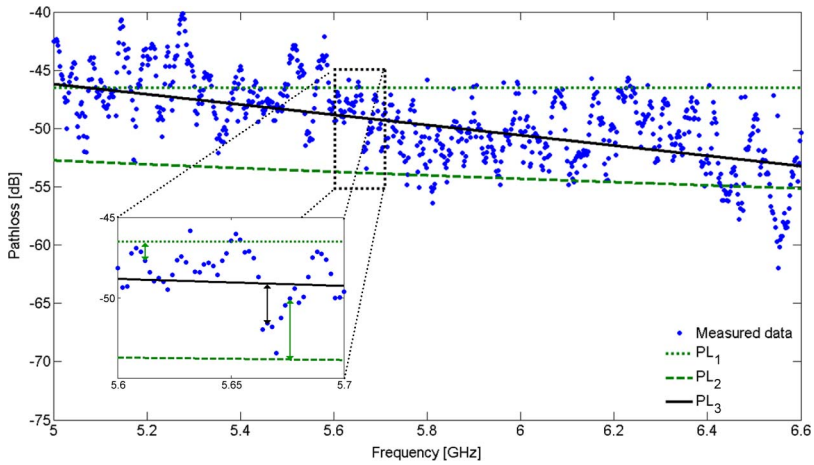

Fig. 7. Graphical representation of PL_i's ($i = 1$, 2, and 3) and their prediction errors at Rx 40 of NLOS.

TABLE IV
PATHLOSS PREDICTION ERRORS OF THREE PATHLOSS FORMULAS DEPENDING ON THE EXISTENCE OF AN LOS PATH

[dB]		$E_f[e_1]$	$E_f[e_2]$	$E_f[e_3]$
LOS	Mean	2.064	6.362	1.610
	Std.	1.15	2.84	1.06
NLOS	Mean	4.057	5.284	3.448
	Std.	2.04	2.15	1.85

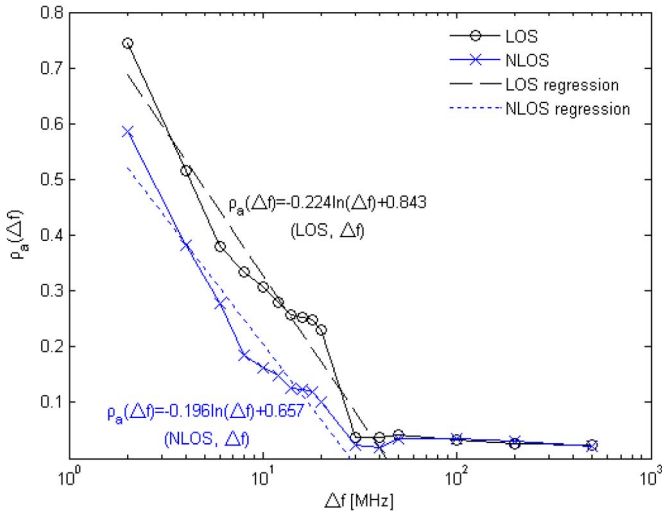

Fig. 8. Correlation coefficients and their linear regression models for the LOS and NLOS locations.

constructed. In all six estimation sets, the reference channel gains are selected for every 10 MHz from set A. Thus

Measured gain set :

$$A = \{a(f_1), \ldots, a(f_k), \ldots, a(f_{801})\}$$

Estimated gain set using linear interpolation :

$$\widetilde{A_L} = \{\tilde{a}_L(f_1), \ldots, \tilde{a}_L(f_k), \ldots, \tilde{a}_L(f_{801})\}$$

Estimated gain set using correlation models :

$$\widetilde{A_j} = \{\tilde{a}_j(f_1), \ldots, \tilde{a}_j(f_k), \ldots, \tilde{a}_j(f_{801})\} \quad (j = 2, 3, \ldots, 6). \tag{11}$$

In the first estimation set $\widetilde{A_L}$, the channel gain element $\widetilde{a_L}(f_k)$ is estimated using the linear interpolation algorithm [22]. The weighting factor for each channel gain at the reference frequency is the frequency separation between the target frequency f_k and the reference frequencies f_{Ri} and $f_{R(i+1)}$. $\widetilde{a_L}(f_k)$ is computed as

$$\widetilde{a_L}(f_k) = \begin{cases} a(f_k), & \text{for } k = 5n+1 \\ & (n = 0, \ldots, 160) \\ \frac{\Delta f_{(i+1)} a(f_{Ri}) + \Delta f_i a(f_{R(i+1)})}{\Delta f_i + \Delta f_{i+1}}, & \text{otherwise.} \end{cases} \tag{12}$$

In (12), f_{Ri} is the closest reference frequency among reference frequencies smaller than f_k, and Δf_i is the frequency separation between f_k and f_{Ri}. Similarly, $f_{R(i+1)}$ is the closest among bigger reference frequencies, and Δf_{i+1} is equal to $(f_{R(i+1)} - f_k)$. In estimated gain sets using correlation models, the channel gains are estimated using the correlation coefficient as follows:

$$\widetilde{a_j}(f_k) = \begin{cases} a(f_k), & \text{for } k = 5n+1 \\ & (n = 0, \ldots, 160) \\ \frac{\sum_{i=1}^{j} \rho_a(\Delta f_i) a(f_{Ri})}{\sum_{i=1}^{j} \rho_a(\Delta f_i)}, & \text{otherwise} \end{cases}$$

$$\text{for } j = 2, 3, \ldots, 6$$

$$\text{where } \rho_a(\Delta f_i) = \rho_{a,\mathrm{LOS(or\ NLOS)}}(\Delta f_i). \tag{13}$$

In these sets, the weighting factors for the channel gains at neighboring reference frequencies are correlation coefficients from (9) in LOS and (10) in NLOS. The index of estimation set j refers to the number of reference channel gains used for the estimation. For example, when j is equal to 3, the channel gain is calculated from the channel gains at three closest reference frequencies. A graphical explanation for the selected estimation sets $\widetilde{A_L}$ and $\widetilde{A_4}$ is illustrated in Fig. 9. In each estimation gain set, the estimation error e_j is defined as the frequency averaged ratio of the absolute value of the difference between

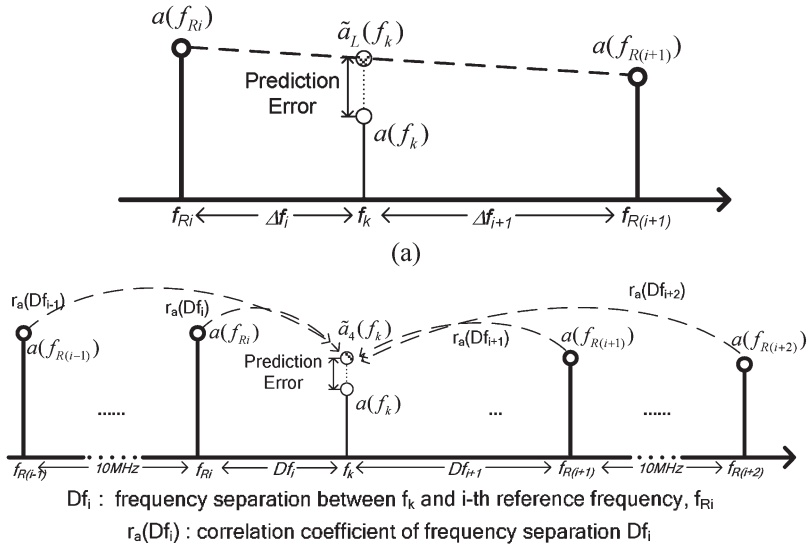

Fig. 9. Graphical expression of the selected channel gain estimation sets $\widetilde{A_L}$ and $\widetilde{A_4}$. (a) Channel gain estimation in the estimation set $\widetilde{A_L}$. (b) Channel gain estimation in the estimation set $\widetilde{A_4}$.

TABLE V
AVERAGE OF THE ESTIMATION ERROR VALUE DEPENDING ON THE EXISTENCE OF LOS WHEN Δf_R IS 10 MHz

		e_L	e_2	e_3	e_4	e_5	e_6
LOS	results	0.111	0.054	0.064	0.071	0.078	0.085
	ratio	1	0.482	0.574	0.639	0.704	0.759
NLOS	results	0.182	0.113	0.127	0.138	0.147	0.155
	ratio	1	0.623	0.696	0.757	0.810	0.854

(ratio)= e_j / e_L (j=L or 2, 3,.., 6)

the measured channel gain and the estimated channel gain to the measured channel gain, i.e.,

$$e_j = E_k\left[\frac{|\widetilde{a_j}(f_k) - a(f_k)|}{a(f_k)}\right] \qquad (j = L \text{ or } 2, 3, \ldots, 6). \tag{14}$$

In (14), to eliminate the effect of the Tx–Rx separation, the absolute difference of the channel gain element is divided by the measured channel gain element. The estimation errors of receiver locations are grouped according to the existence of a LOS path and summarized in Table V. The ratio in Table V is the relative performance of the estimation using correlation models compared to that using the linear interpolation algorithm.

In both the LOS and NLOS locations, e_2 is the smallest. In particular, with a LOS path, the estimation error of the linear interpolation estimation is reduced by about 50% when the channel gains are estimated from channel gains at two closest reference frequencies. As channel gains are more correlated in LOS locations, the estimation algorithm using correlation models has better performance when the LOS path is guaranteed. In addition, it is found that the estimation using correlation models has the best performance when j is equal to 2. Although more channel gain information is added with increasing j, the estimation error increases rather than decreases because the correlation coefficients between the target channel gain and the added channel gains are too small to make the estimation accurate.

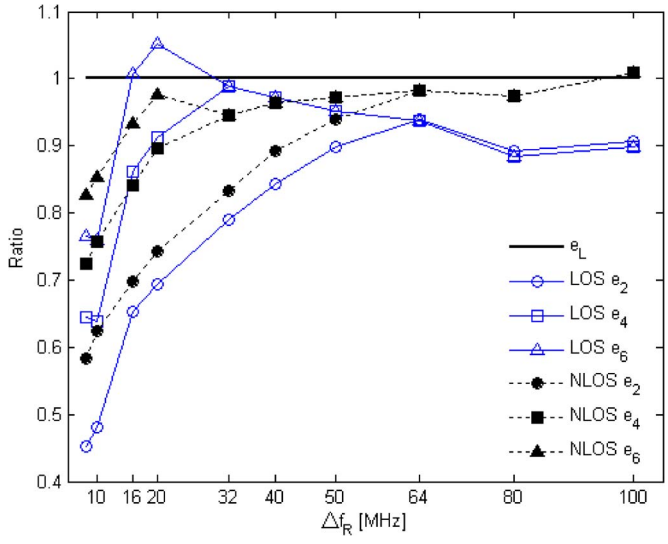

Fig. 10. Variation of the ratio between e_L and e_j's (j = 2, 4, and 6) with an interval between reference frequencies.

TABLE VI
AVERAGE OF THE ESTIMATION ERROR VALUE DEPENDING ON THE EXISTENCE OF LOS

	Δf_R	8	10	20	40	64	100
LOS	e_L	0.091	0.111	0.170	0.250	0.297	0.370
	e_2	0.041	0.054	0.117	0.208	0.270	0.326
	Ratio	0.45	0.48	0.69	0.83	0.91	0.88
NLOS	e_L	0.143	0.182	0.281	0.411	0.431	0.487
	e_2	0.083	0.113	0.225	0.394	0.418	0.526
	Ratio	0.58	0.62	0.73	0.88	0.97	1.02

So far, the interval between reference frequencies is fixed to 10 MHz. However, the performance of the estimation algorithm is changed due to the variation of the interval between reference frequencies Δf_R. In Fig. 10, the variation of the ratio between e_L and e_j's $(j = 2, 4, 6)$ to Δf_R is illustrated, whereas absolute values of e_L and e_2 are summarized in Table VI. As shown in Fig. 10, the relative accuracy of the estimation using correlation models decreases as Δf_R increases. For example, the ratio between e_L and e_2, which is about 0.5 with a 10-MHz Δf_R, becomes about 0.9 when Δf_R is bigger than 50 MHz. This is because the estimation using the correlation model becomes ineffective as the correlation coefficient becomes smaller with increasing Δf_R.

In Table VI, it is found that to guarantee the estimation error lower than 20%, Δf_R is set to 25 MHz with the LOS path and to 12 MHz without the LOS path when the linear interpolation algorithm is applied. Once the correlation model is applied to the estimation, however, Δf_R's can be expanded as 36 MHz for LOS and 18 MHz for NLOS, which means that the number of reference frequencies in the given frequency band is reduced as the correlation model is used in the frequency-domain channel gain estimation.

V. CONCLUSION

For efficient UWB systems engineering, we have proposed a frequency-dependent empirical UWB channel model for office environments. The measurements were performed at 103 receiver locations of six receiver groups using the frequency sweep method. From the results, the pathloss exponent variation with frequency was modeled as a linear function of frequency, and the difference between the maximum and minimum values of the pathloss exponent for a 500-MHz frequency band was proportional to the pathloss exponent value of the overall frequency band. Using this pathloss exponent variation model, pathloss prediction can more accurately be performed than is possible using existing pathloss formulas. For characterization of the UWB correlation property, the correlation coefficient was represented as a linear regression model with a double slope that depends on the existence of an LOS path. Using this correlation coefficient modeling, the unknown channel gains of intervening frequencies are estimated from known channel information of reference frequencies. Through the performance variation analysis of the number of the reference frequency and the interval between the reference frequency, it is confirmed that estimation using the correlation property from known channel gain information of two closest frequencies has the best estimation accuracy as it decreases the estimation error by about 50% with the LOS path and by 40% without the LOS path when the interval between the reference frequency is 10 MHz.

REFERENCES

[1] Fed. Commun. Comm., *First Order and Report, Revision of Part 15 of the Commission's Rules Regarding UWB Transmission Systems*, Apr. 2002. FCC 02-48.

[2] A. F. Molisch, J. R. Foerster, and M. Pendergrass, "Channel models for ultrawideband personal area networks," *IEEE Trans. Wireless Commun.*, vol. 10, no. 6, pp. 14–21, Dec. 2003.

[3] A. F. Molisch, K. Balakrishnan, D. Cassioli, C.-C. Chong, S. Emami, A. Fort, J. Karedal, J. Kunisch, H. Schantz, U. Schuster, and K. Siwiak, "IEEE 802.15.4a channel model—Final report," Tech. Rep. Doc. IEEE 802.15-04-0662-02-004a, 2005.

[4] D. Cassioli, M. Z. Win, and A. F. Molisch, "The ultra-wide bandwidth indoor channel: From statistical model to simulations," *IEEE J. Sel. Areas Commun.*, vol. 20, no. 6, pp. 1247–1257, Aug. 2002.

[5] K. Siwiak, "A path link model for ultra wide band pulse transmissions," in *Proc. IEEE VTC Spring*, May 2001, vol. 2, pp. 1173–1175.

[6] S. S. Ghassemzadeh, L. J. Greenstein, A. Kavcic, T. Sveinsson, and V. Tarokh, "UWB indoor pathloss model for residential and commercial buildings," in *Proc. IEEE VTC Fall*, Oct. 2003, vol. 5, pp. 3115–3119.

[7] B. Uguen, E. Plouhinec, Y. Lostanlen, and G. Chassay, "A deterministic ultra wideband channel modeling," in *Proc. IEEE Conf. Ultra Wideband Syst. Technol.*, May 2002, pp. 1–5.

[8] J. Choi, N.-G. Kang, Y.-S. Sung, and S.-C. Kim, "Empirical ultra wide band pathloss model in office environments," in *Proc. IEEE VTC Spring*, May 2006, vol. 4, pp. 1956–1960.

[9] C. C. Chong and S. K. Yong, "A generic statistical-based UWB channel model for high-rise apartments," *IEEE Trans. Antennas Propag.*, vol. 53, no. 8, pp. 2389–2399, Aug. 2005.

[10] C. C. Chong, Y. E. Kim, S. K. Yong, and S. S. Lee, "Statistical characterization of the UWB propagation channel in indoor residential environments," *Wireless Commun. Mobile Comput.*, vol. 5, no. 5, pp. 503–512, Aug. 2005.

[11] R. C. Qiu and I. T. Lu, "Wideband wireless multipath channel modeling with path frequency dependence," in *Proc. IEEE ICC*, Dallas, TX, Jun. 1996, pp. 277–281.

[12] R. C. Qiu and I. T. Lu, "Multipath resolving with frequency dependence for broadband wireless channel modeling," *IEEE Trans. Veh. Technol.*, vol. 48, no. 1, pp. 273–285, Jan. 1999.

[13] K. Makaratat and S. Stavrou, "Spatial correlation technique for UWB antenna arrays," *Electron. Lett.*, vol. 42, no. 12, pp. 675–676, Jun. 2006.

[14] K. Witrisal and M. Pausini, "Statistical analysis of UWB channel correlation functions," *IEEE Trans. Veh. Technol.*, vol. 57, no. 3, pp. 1359–1373, May 2008.

[15] I. Oppermann, M. Hämälainen, and J. Iinatti, "UWB channel models," in *UWB Theory and Applications*. Chichester, U.K.: Wiley, 2004.

[16] W. Sorgel and W. Wiesbeck, "Influence of the antennas on the ultra-wideband transmission," *EURASIP J. Appl. Signal Process.*, vol. 2005, no. 3, pp. 296–305, 2005.
[17] T. S. Rappaport, "Mobile radio propagation: Large-scale pathloss," in *Wireless Communications: Principles and Practice*, 2nd ed. Englewood Cliffs, NJ: Prentice–Hall, 2002.
[18] J. R. Andrews, "UWB signal sources, antennas & propagation," in *Proc. IEEE Top. Conf. Wireless Commun. Technol.*, Oct. 2003, pp. 439–440.
[19] MBOA, *MultiBand OFDM Physical Layer Proposal for IEEE Task Group 3a*, Sep. 2004. [Online]. Available: http://www.wimedia.org
[20] J. D. Parsons, "Fundamentals of VHF and UHF propagation," in *The Mobile Radio Propagation Channel*, 2nd ed. New York: Wiley, 2000.
[21] A. Leon-Garcia, "Random processes," in *Probability and Random Processes for Electrical Engineering*, 2nd ed. Reading, MA: Addison-Wesley, 1994.
[22] S. M. Kay, "Linear bayesian estimators," in *Fundamentals of Statistical Signal Processing: Estimation Theory*. Englewood Cliffs, NJ: Prentice–Hall, 1993.

Jinwon Choi (S'08) received the B.S and Ph.D. degrees in electrical engineering from Seoul National University, Seoul, Korea, in 2002 and 2009, respectively.

His current research areas are ultrawideband channel characterization, wireless sensor networks, and systems engineering of wireless systems.

Noh-Gyoung Kang received the B.S., M.S., and Ph.D. degrees from Seoul National University, Seoul, Korea, in 2000, 2002, and 2007, respectively, all in electrical engineering.

Since 2007, he has been with Samsung Electronics Co., Suwon, Korea. His current research area is ultrawideband channel characteristics near the body area.

Yu-Suk Sung received the B.S. and M.S. degrees in electrical engineering in 2003 and 2006, respectively, from Seoul National University, Seoul, Korea, where he is currently working toward the Ph.D. degree.

His current research areas are performance analysis and systems engineering of wireless systems.

Jun-Sung Kang received the B.S. and M.S. degrees in electrical engineering from Seoul National University, Seoul, Korea, in 2006 and 2009, respectively.

His current research area is ultrawideband channel characteristics near the body area.

Seong-Cheol Kim (S'91–M'96) received the B.S. and M.S. degrees in electrical engineering from Seoul National University, Seoul, Korea, in 1984 and 1987, respectively, and the Ph.D. degree in electrical engineering from Polytechnic University, Brooklyn, NY, in 1995.

From 1995 to 1999, he was with the Wireless Communications Systems Engineering Department, AT&T Bell Laboratories, Holmdel, NJ. Since 1999, he has been with Department of Electrical Engineering and Computer Science, Seoul National University, as a Professor. He has authored more than 30 journal papers and 38 international conference papers. His current research area covers multiple-input–multiple-output (MIMO) channel modeling, ultrawideband channel modeling, MIMO orthogonal frequency division multiplexing systems, femtocell algorithm development, self-heterodyne receivers, power line communication, and systems engineering of wireless systems.